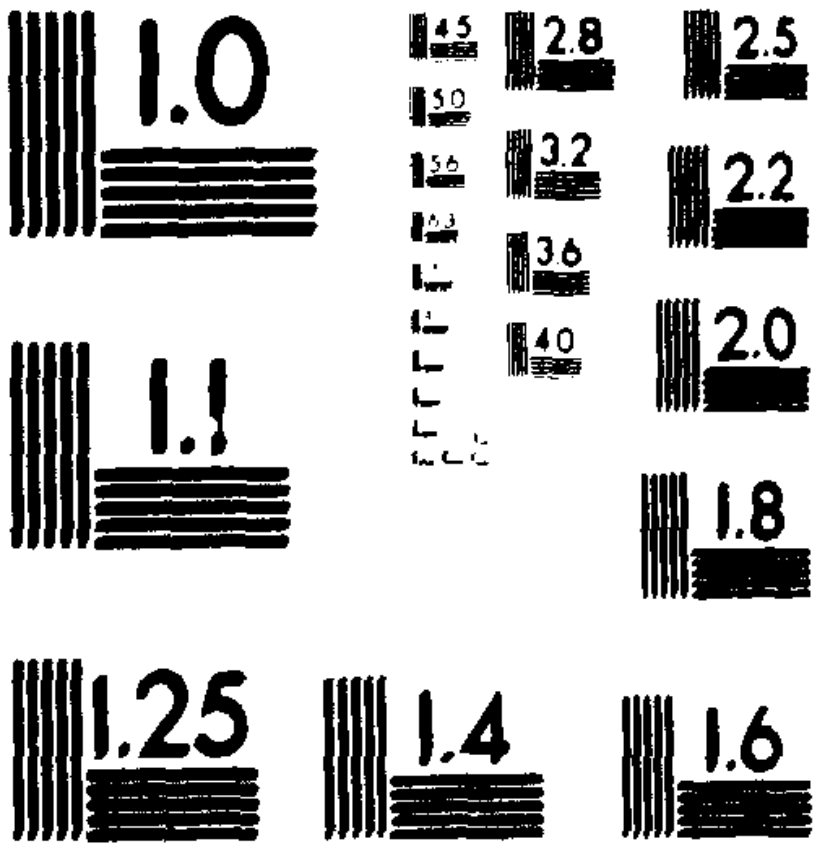

ISSN/0393-6333

RT/TIB/86/44

F. CIOCCI, G. DATTOLI, A. DORIA, G. SCHETTINI, A. TORRE, J.E. WALSH

SPONTANEOUS EMISSION IN CERENKOV FEL DEVICES: A PRELIMINAR THEORETICAL AND EXPERIMENTAL ANALYSIS

COMITATO NAZIONALE PER LA RICERCA E PER LO SVILUPPO DELL'ENERGIA NUCLEARE E DELLE ENERGIE ALTERNATIVE

ISSN/0393-6333

COMITATO NAZIONALE PER LA RICERCA E PER LO SVILUPPO
DELL'ENERGIA NUCLEARE E DELLE ENERGIE ALTERNATIVE

SPONTANEOUS EMISSION IN CERENKOV FEL DEVICES: A PRELIMINAR THEORETICAL AND EXPERIMENTAL ANALYSIS

F. Ciocci, G. Dattoli
ENEA-Dipartimento Tecnologie Intersettoriali di Base, Centro ricerche energia Frascati

A. Doria, G. Schettini
ENEA Student

A. Torre
Dipartimento di Fisica, Università di Salerno and ENEA Guest

J.E. Walsh
Department of Physics and Astronomy, Dartmonth College, Hanover, NH. 03755 (USA)

RT/TIB/86/44

Testo pervenuto nel novembre 1986

SUMMARY

The main features of the spectral characteristics of the spontaneously emitted Cerenkov light in circular and rectangular wave-guides filled with dielectric are discussed. The characteristics of the radiation emitted by an electron beam moving near and parallel to the surface of a dielectric slab are also analysed. Finally, the relevance of these results to a possible FEL-Cerenkov operation is briefly discussed.

RIASSUNTO

In questo lavoro vengono discusse le caratteristiche dello spettro della radiazione Cerenkov, emessa in guide d'onde circolari e rettangolari riempite con dielettrico. Si analizzano inoltre le proprietà della radiazione emessa da un fascio di elettroni in moto in prossimità e parallelamente alla superficie di una "slab" di dielettrico. Si discute, infine, brevemente, l'importanza di questi risultati per la realizzazione di un possibile FEL-Cerenkov.

I. INTRODUCTION

In the most widespread Free Electron Laser (FEL) devices, an ultrarelativistic e-beam is injected in an undulator magnet where it generates a light pulse, which, stored in an optical cavity, reinteracts with a new copropagating e-beam and results amplified by the mechanism of stimulated emission [1].

A large number of magnetic undulator FEL's has been so far designed and many of them have been succesfully operated [2].

The degree of maturity of this new source of coherent radiation is enough developed to make the FEL a "tool" for many scientific applications [3]. It has, indeed, been shown that an FEL can be operated with "low technology" accelerators [4], thus considerably reducing all the construction and management costs [5].

Even though magnetic undulator based FEL's have reached so significant achievements, free electron coherent sources based on different emission mechanisms have been proposed. In particular the possibility of operating Cerenkov [6] or Smith-Purcell [7] FEL's has been thouroughly investigated [8]. Attempts to enhance the Cerenkov radiation power by prebunching the electrons in the beam were accomplished more than two decades ago [9]. The power, however, remained small since there was no reinforcement of the bunching by an internal feedback mechanism. More recently the possibility of producing intense low-energy e.b. has provided strong radiation from stimulated Cerenkov effect [10,11].

In particular the results obtained at Dartmouth have shown that this effect may be a remarkable FEL source in the millimiter and submillimeter wave-length region [12]. Furthermore the possibility of getting radiation at shorter wave-lengths has been theoretically investigated [13] and preliminar comparisons have shown that a Cerenkov based FEL (C-FEL) may provide, in the far infrared region, a moderate power compact laser device, with better performances than an undulator FEL (U-FEL) [14].

In a C-FEL (for the details of the experimental proposals see Ref. 15) the e.b. moves near and parallel to the surfaces of a dielectric resonator (see Fig. 1), the presence of the dielectric reduces the speed of the radiation thus allowing a synchronous coupling of the e-beam to the axial component of a TM mode and therefore causing spontaneous Cerenkov radiation emission in a bounded structure. In

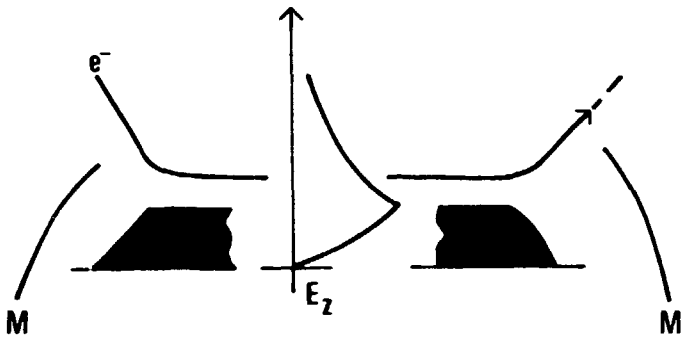

Fig. 1 C-FEL configuration

principle, whenever the gain is sufficient, the addition of mirrors provides the condition to get an oscillator. In the following we will discuss the mechanism of frequency selection determined by the velocity synchronism of the e-beam and the guided mode.

Although much theoretical effort has been devoted to elucidate the gain mechanism and to put in evidence the possible advantages of a C-FEL with respect to an U-FEL, the detailed analysis of the spontaneous emission in structures of relevance to a C-FEL device have not been so far accomplished. Since the spontaneous emission effect is the pre-requisite for the onset of the laser radiation we believe that a deeper analysis of the characteristics of the spectral features of the spontaneous radiation is necessary for a more complete theoretical understanding of the C-FEL process.

We stress that a careful understanding of the spontaneous emission in undulator magnets has indicated the possibility of using the emitted light in a more flexible way, exploiting e.g. the odd harmonics on-axis emission in a planar undulator or the off-axis higher harmonics to get a larger tunability range of the laser [16]. Similar considerations, mutatis mutandis, may apply to the C-FEL too. In this paper we address the question of calculating the Cerenkov spontaneous emission spectra in the three possible configurations: circular and rectangular wave-guides filled with dielectric and plane wave-guide with a dielectric surface (slab).

The paper is organized as follows: section 2 is devoted to general considerations on the calculation scheme, in section 3 we specialise the previous results to the spectra of the radiation

emitted in circular and rectangular wave-guides, the slab configuration is discussed in section 4, finally section 5 is devoted to conclusive remarks.

II. GENERAL FORMULATION

As already stated, the purpose of the paper is the analysis of the characteristics of the radiation emitted by an e-beam in uniform motion inside and near a dielectric in a wave-guide whose geometry will be specified later.

The analysis we develope closely follows the method utilised more than thirty years ago by Linhart [17] who calculated the radiation emitted by a point-like charge in uniform motion on a straight line parallel to the plane face of a semi-infinite dielectric slab. For the sake of completness we must stress that a similar technique has been also applied to the study of the Cerenkov radiation in periodic linear structures [18]. In absence of charges the field in the wave-guide can be represented in the form

$$\vec{A}(r, t) = \sum_{\lambda} e^{i\omega_\lambda t} \vec{A}_\lambda(r) \tag{2.1}$$

where the subscript λ is a parameter denoting the various e.m. waves which can oscillate at frequency ω_λ in the structure when no charges are present.

The field produced by a charge moving along the structure may be conveniently expanded according to the relation

$$\vec{A}(r,t) = \sum_{\lambda} q_\lambda(t)\, \vec{A}_\lambda(r) \tag{2.2}$$

where the time-dependent coefficients $q_\lambda(t)$, still to be determined, contain all the features of the λ-th mode evolution. Since $\vec{A}_\lambda(r)$ is a solution of the field equations in absence of charges, the expansion (2.2) correctly describes the transverse part of the vector potential only. This is however sufficient for our purposes, since we are interested in the evolution of the radiation field only.

The spatial part of (2.2) specialises to

$$\vec{A}_\lambda(r) = \vec{s}_\lambda(r) \sin(kz) \tag{2.3}$$

for a wave-guide structure with plane-conducting surfaces at z = 0, L and k is a discrete parameter given by

$$k = \frac{n\pi}{L} \quad , \qquad n = 0, \pm 1, \pm 2..... \tag{2.4}$$

The explicit time-behaviour of the λ-th mode will be obtained by solving the equation of motion for $q_\lambda(t)$ given by [19]

$$\ddot{q}_\lambda(t) + \omega_\lambda^2 \, q_\lambda(t) = 1/c \int_v \vec{j} \cdot \vec{A}_\lambda^* \, dv \tag{2.5}$$

with initial conditions $q_\lambda(o) = \dot{q}_\lambda(o) = 0$, sufficient to describe the "start-up" of the radiation from the vacuum. Equation (2.5) describes the evolution of the e.m. field driven by a point-like charge, with an associated current density $\vec{j}$, in terms of a forced harmonic oscillator with a force term

$$F_\lambda(t) = 1/c \int_v \vec{j} \cdot \vec{A}_\lambda^* \, dv \tag{2.6}$$

The frequency spectrum of $F_\lambda(t)$ is specified by the Fourier-transform of (2.6)

$$\tilde{F}_\lambda(\omega) = \frac{1}{2\pi} \int_{-\infty}^{+\infty} F_\lambda(t) \, e^{-i\omega t} \, dt \tag{2.7}$$

the current density $\vec{j}$ can be written for a point-like charge q in uniform motion as

$$\vec{j}\,(r,t) = q\vec{v} \; \delta(x-x_e) \; \delta(y-y_e) \cdot \delta(z-c\beta_o t) \; \theta(t)\theta(L/c\beta_o - t) \tag{2.8}$$

where θ and δ are the Heaviside and Dirac functions, respectively, $x_e(t)$, $y_e(t)$ and $z_e(t) = c\beta_o t$ ($\beta_o = v_z/c$) are the instantaneous coordinates of the charge. The structure of (2.8) reflects the fact that the interaction has a finite duration (L ≡ length of the interaction region).

Combining (2.8) and (2.6) one gets the following expression for the driving-force term

$$F_\lambda(t) = f_\lambda(t) \sin(ck\beta_o t) \tag{2.9}$$

where

$$f_\lambda(t) = q\,\vec{\beta}\cdot\vec{a}_\lambda(x_e(t),\, y_e(t),\, c\beta_o t)\;\theta(t)\;\theta(L/c\beta_o - t)$$
$$\vec{\beta} = \vec{v}/c \tag{2.10}$$

The Fourier-Transform (2.7) can be easily calculated and reads

$$\tilde{F}_\lambda(\omega) = -\,i/2\,\{\tilde{f}_\lambda(\omega - ck\beta_o) - \tilde{f}_\lambda(\omega + ck\beta_o)\} \tag{2.11}$$

The solution of Eq. (2.5) can be easily found and, for the given initial conditions, can be written in the form

$$q_\lambda(t) = \int_{-\infty}^{+\infty} \frac{\tilde{F}_\lambda(\omega)}{\omega_\lambda^2 - \omega^2}\, e^{i\omega t}\, d\omega \tag{2.12}$$

The energy per mode stored in the wave-guide is given by

$$\mathcal{E}_\lambda = 1/2\,[|\dot{q}_\lambda|^2 + \omega_\lambda^2\,|q_\lambda|^2] \tag{2.13}$$

therefore the rate of energy exchange between the electron and fields can be calculated from (2.13) and reads:

$$d\mathcal{E}_\lambda/dt = 1/2\;\mathrm{Re}\;[F_\lambda^*(t)\cdot\dot{q}_\lambda(t)] \tag{2.14}$$

The integration of (2.14) over the interaction region yields the total amount of power delivered by the electron, namely

$$\mathcal{E} = 1/4\;\mathrm{Re}\;\{\Sigma_\lambda\; i\int_{-\infty}^{+\infty} F_\lambda^*(t)\;[\int_{-\infty}^{+\infty} \frac{\tilde{F}_\lambda(\omega)}{\omega_\lambda - \omega}\, e^{i\omega t} d\omega - \int_{-\infty}^{+\infty} \frac{\tilde{F}_\lambda(\omega)}{\omega_\lambda + \omega}\, e^{i\omega t} d\omega]dt\} \tag{2.15}$$

A more convenient way of rewriting (2.15) is the elimination of the sum over the index λ, via a substitution with an integration over the continuous variable k and a sum over the set of the discrete indices $\{s\}$ characterising the mode. The price to be payed is the introduction of a "k - density" function $\bar{\rho}_k[\{s\},\omega]$, while the gained advantage results in the possibility of getting for (2.15) the simpler form

$$\mathcal{E} = \int d\omega \sum_{\{s\}} \frac{\pi^2}{c} \frac{|\tilde{F}\{s\}(\omega)|^2}{[d/dk\;(\omega_{[k,\{s\}]}/c) - \beta_o]}\, \bar{\rho}_k\,(\{s\},\omega)\Big|_{\omega_{[k,\{s\}]}=\omega} \tag{2.16}$$

The results obtained in this section are the necessary mathematical background to study the basic features of the spontaneous emission in a C-FEL device. However we also stress that they can be envisaged as the first step of a self-consistent analysis of the laser signal growth as developed in Ref. 20.

III. CIRCULAR AND RECTANGULAR WAVE-GUIDE CONFIGURATIONS

The formalism developed in the previous section will be utilised to carry out a numerical investigation of the spectral properties of the Cerenkov radiation emitted in a circular and rectangular wave-guide filled with dielectric.

IIIa) Circular geometry.

We consider a circular wave-guide with radius a, filled with a dielectric of constant ε and with a total length L, closed by plane conducting surfaces at Z=0,L (see Fig. 2).

In this case the current density for a particle moving in the plane $\phi=\phi_0$ with longitudinal and transverse velocity $\beta_0 c$ and $\beta_\perp c$ respectively, can be characterized by a set of cylindrical coordinates

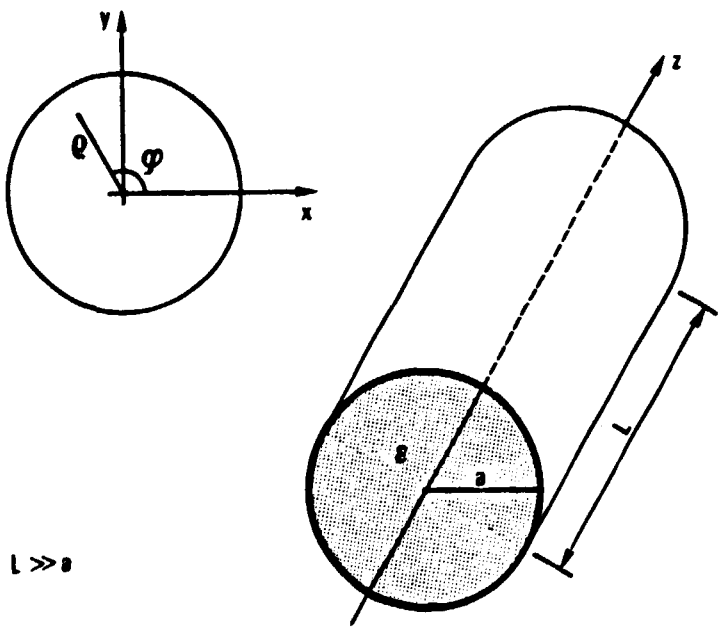

Fig. 2 Circular geometry.

$$\vec{j} \equiv (j_\rho, j_\phi, j_z) \tag{3.1}$$

whose components explicitely read

$$j_\rho = qc/\rho\ \beta_\perp\ \delta[\rho-(\rho_o+c\beta_\perp t)]\ \delta(z-c\beta_o t)\ \delta(\phi-\phi_o)\ \theta(t)\ \theta(L/c\beta_o-t)$$

$$j_\phi = 0 \tag{3.2}$$

$$j_z = qc/\rho\ \beta_o\ \delta[\rho-(\rho_o+c\beta_\perp t)]\ \delta(z-c\beta_o t)\ \delta(\phi-\phi_o)\ \theta(t)\ \theta(L/c\beta_o - t)$$

According to the cylindrical symmetry involved the modes can be characterised by three parameters [21], namely $\lambda \equiv [k,(n,m)]$, where n and m specify the $TM_{n,m}$ modes. Considering a particle moving parallel to the z-axis ($\beta_\perp = 0$), the force term (2.10) takes the form

$$f_\lambda(\rho,t) = q\beta_o\ B_{n,m}\ J_n\ (p\rho)\ \theta(t)\ \theta(L/c\beta_o - t) \tag{3.3}$$

where $J_n(x)$ is the n-th Bessel function of the first kind, p and $B_{n,m}$ are defined by

$$p^2 = (\frac{\omega}{c})^2\ \varepsilon - k^2$$

$$B^2_{n,m} = (\frac{8}{L})\ \frac{c^4}{\varepsilon^2}\ \frac{\mu^2_{n,m}}{a^4}\ \frac{1}{\omega^2[J'_n(\mu_{n,m})]^2} \tag{3.4}$$

and $\mu_{n,m}$ is the m-th zero of the Bessel function J_n.

We can evaluate, using the above formulas and (2.16), the energy radiated per unit frequency-bandwidth as

$$\frac{d\mathcal{E}}{d(\omega/c)} = -\frac{q^2L^2}{2\pi\varepsilon^2a^5(\omega/c)^2} \sum_{\mu_{n,m}\leq\sqrt{\varepsilon}a(\omega/c)} \mu^3_{n,m}\ [\frac{J_n(\mu_{n,m}\ (\rho_o/a)}{J'_n(\mu_{n,m})}]^2 \cdot$$

$$\cdot\ [(\frac{\sin\theta_-}{\theta_-})^2 + (\frac{\sin\theta_+}{\theta_+})^2 - 2(\frac{\sin\theta_-}{\theta_-})(\frac{\sin\theta_+}{\theta_+})\ \cos kL] \cdot$$

$$\cdot\ [\frac{1}{(k/\varepsilon(\omega/c)-\beta_o)k}]\Big|_{k=(\omega^2\varepsilon/c^2-\mu^2_{n,m}/a^2)^{1/2}} \tag{3.5}$$

where the angles $\theta_{\mp}$ are defined by

$$\theta_{\mp} = [k\beta_o \mp (\omega/c)]\ L/2\beta_o \qquad (3.6)$$

The frequency selection can be understood, at least qualitatively, from eqs. (3.5,6). One will, indeed, obtain a number of peaks centered around the zeros of $\theta_{\pm}$ with the characteristic sinc-shape. The condition $\theta_{\pm}=0$ realizes the so called phase-matching or synchronism condition which allows energy transiering from the electron to the radiation field (or viceversa for an already preexisting radiation mode in the resonator). As already stated from $\theta_{\pm}= 0$ we get the wave-length at which emission should be expected we also stress that the same condition can be derived from simple kinematic considerations without involving the cumbersome analysis so far developed [22].

The relation (3.5) accounts for the energy transfer from one--single electron, to treat the more realistic case of e-beam configuration a convolution of (3.5) on the initial transverse beam distribution is needed. The results of the numerical analysis are shown in Fig. 3 where (3.5) has been plotted for different values of the interaction length (a=0.5 cm, β_o=0.95).

When L is enough large there is a clear selection of two modes and indeed the sinc is well approximated by a Dirac-function (see Fig. 3a). For decreasing L (Fig. 3b) a natural line broadening arises, together with an interference between the side--bands of the sinc-functions.

The off-axis emission ($\rho_o \neq 0$) is shown in Fig. 4 and the remarkable feature is a third peak appearing in between the two previous "strong modes". For shorter values of the interaction length the presence of the third peak is smoothed by the interference.

An idea of the shape of the emission line is given in Fig. 5 where we present an enlarged view of the mode both on and off axis.

IIIb) Rectangular geometry

The case discussed in this section is a straightforward extension of the previously analysed configuration.

Referring to Fig. 6 the relevant dispersion relations write [21]

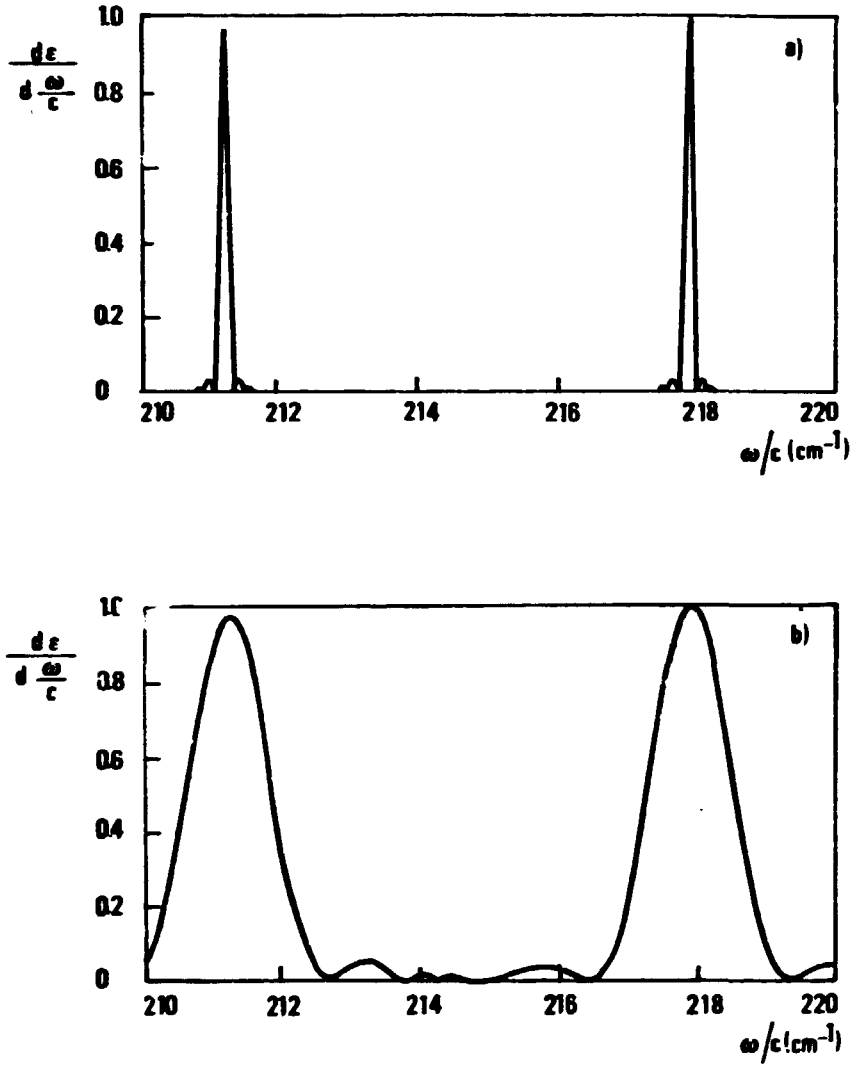

Fig. 3 On axis spectrum for a circular waveguide: (a) the sinc-functions are well distinguished (L=50 cm; $[d\ /d(\omega/c)]_{max}$ = = 0.89 x 10^{-14} erg x cm; (b) for shorter interaction length an interference arises between the two modes (L=5 cm; $[d\ /d(\omega/c)]_{max}$ = 0.90 x 10^{-16} erg x cm).

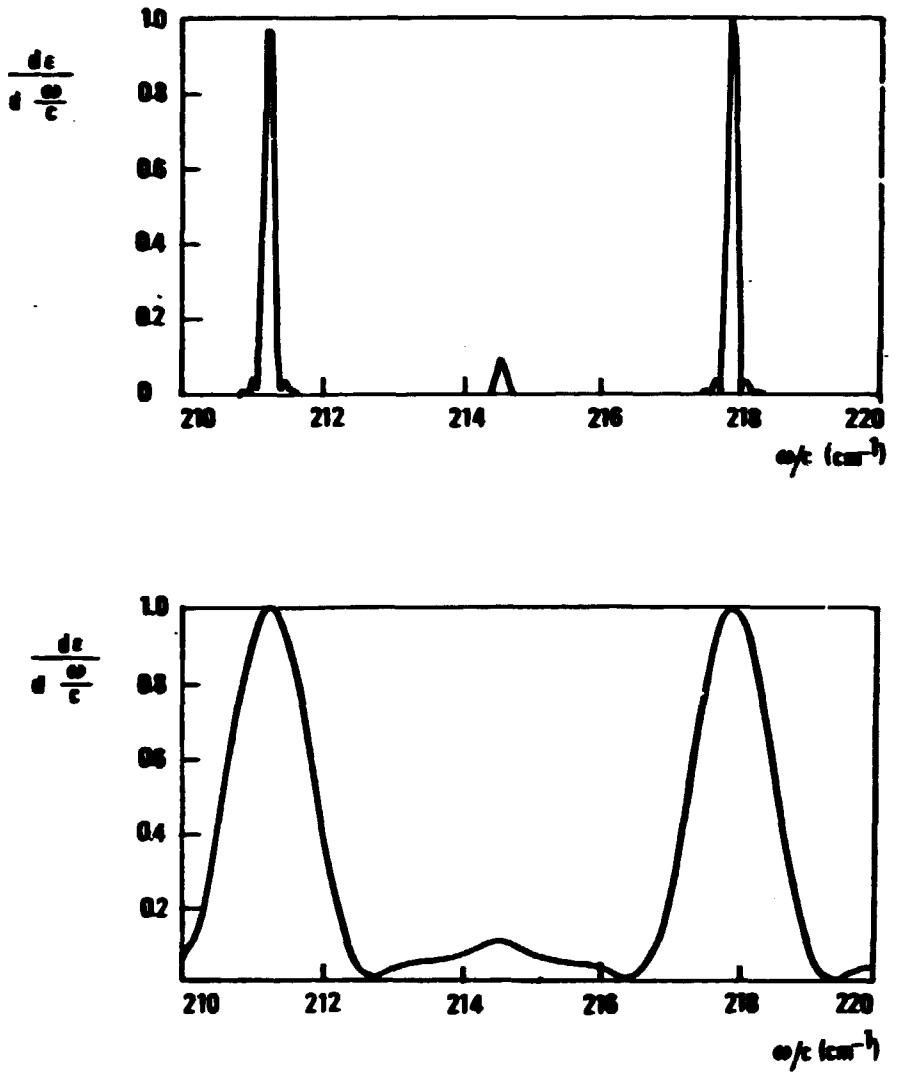

Fig. 4 Off-axis spectrum for a circular waveguide ($\rho_o/a=0.01$). The number of excited modes is increased.
(a) L=50 cm; $[d\ /d(\omega/c)]_{max} = 0.44 \times 10^{-14}$ erg x cm).
(b) L=5 cm; $[d\ /d(\omega/c)]_{max} = 0.53 \times 10^{-16}$ erg x cm).

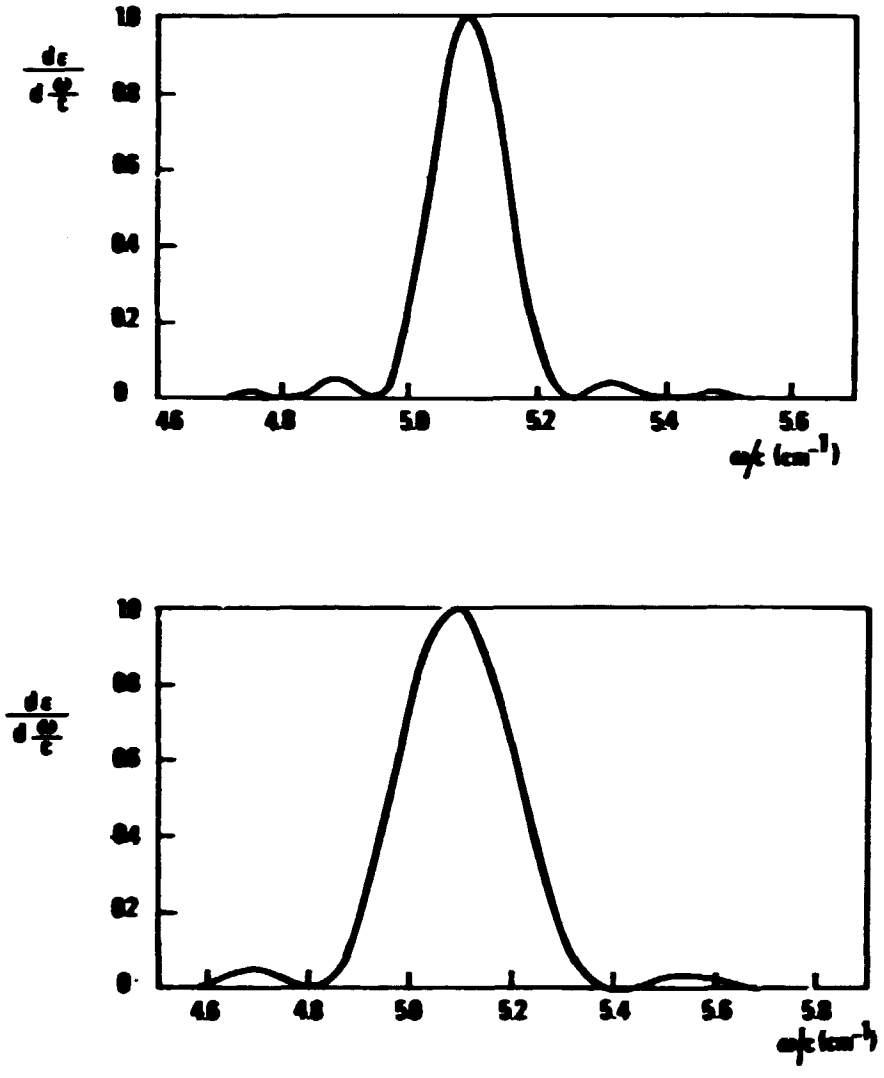

Fig. 5 Enlarged view of an excited mode: (a) on-axis, (b) off-axis.

$$\varepsilon\left(\frac{\omega}{c}\right)^2 - k^2 = \gamma_{mn}^2 \tag{3.7}$$

where

$$\gamma_{mn}^2 = \left[\left(\frac{m\pi}{a}\right)^2 + \left(\frac{n\pi}{b}\right)^2\right] \tag{3.8}$$

is the transverse wave-number.

The current density in cartesian coordinates reads

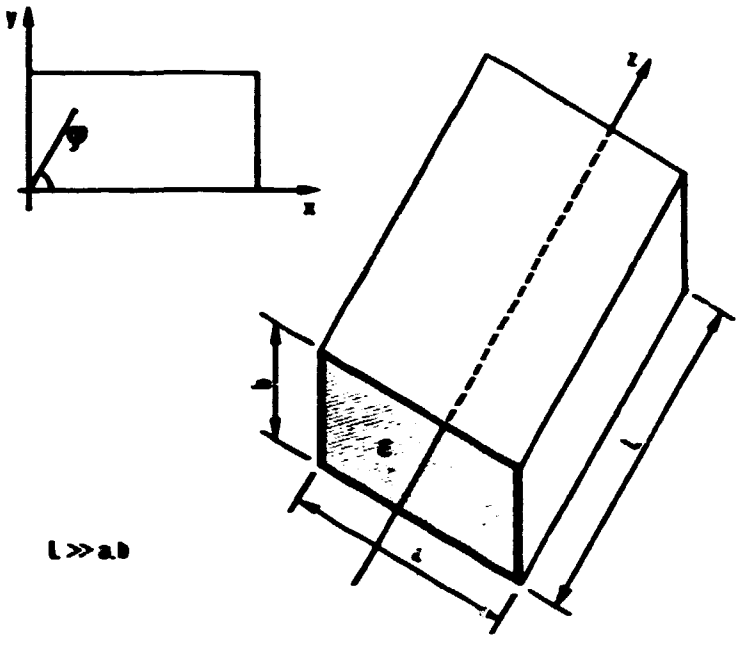

Fig. 6 Rectangular geometry.

$$\vec{j}(r,t) = q[c\beta_\perp \cos\phi_o\, \hat{x} + c\beta_\perp \sin\phi_o\, \hat{y} + c\beta_o\, \hat{z}]\, \delta(x-x_e)\delta(y-y_e)\, \delta(z-c\beta_o t) \cdot \theta(t)\, \theta(L/c\beta_o - t) \tag{3.9}$$

Without reporting, the otherwise straightforward, intermediate steps, already stated in 3a, the energy per unit bandwidth can be written as

$$\frac{d\mathcal{E}}{d(\omega/c)} = -\frac{2e^2L^2}{\varepsilon ab} \sum_{m,n} \sin^2\left(\frac{m\pi}{a} x_e\right) \sin^2\left(\frac{n\pi}{b} y_e\right) \cdot \frac{\gamma_{mn}^2}{k^2+\gamma_{mn}^2} \cdot \left\{\left(\frac{\sin\theta_-}{\theta_-}\right)^2 + \left(\frac{\sin\theta_+}{\theta_+}\right)^2 - 2\left(\frac{\sin\theta_-}{\theta_-}\right)\left(\frac{\sin\theta_+}{\theta_+}\right)\cos(kL)\right\} \cdot \frac{1}{[k/\varepsilon(\omega/c)-\beta_o]k} \tag{3.10}$$

with the same previous definition of $\theta_{\pm}$.

Furthermore the sum over the indices m,n runs in such a way that $\gamma_{mn} < \sqrt{\varepsilon}\, m/c$ [21].

The same considerations developed in the previous subsection apply to (3.10).

In Fig. 7 we report the emission spectra for the particle moving

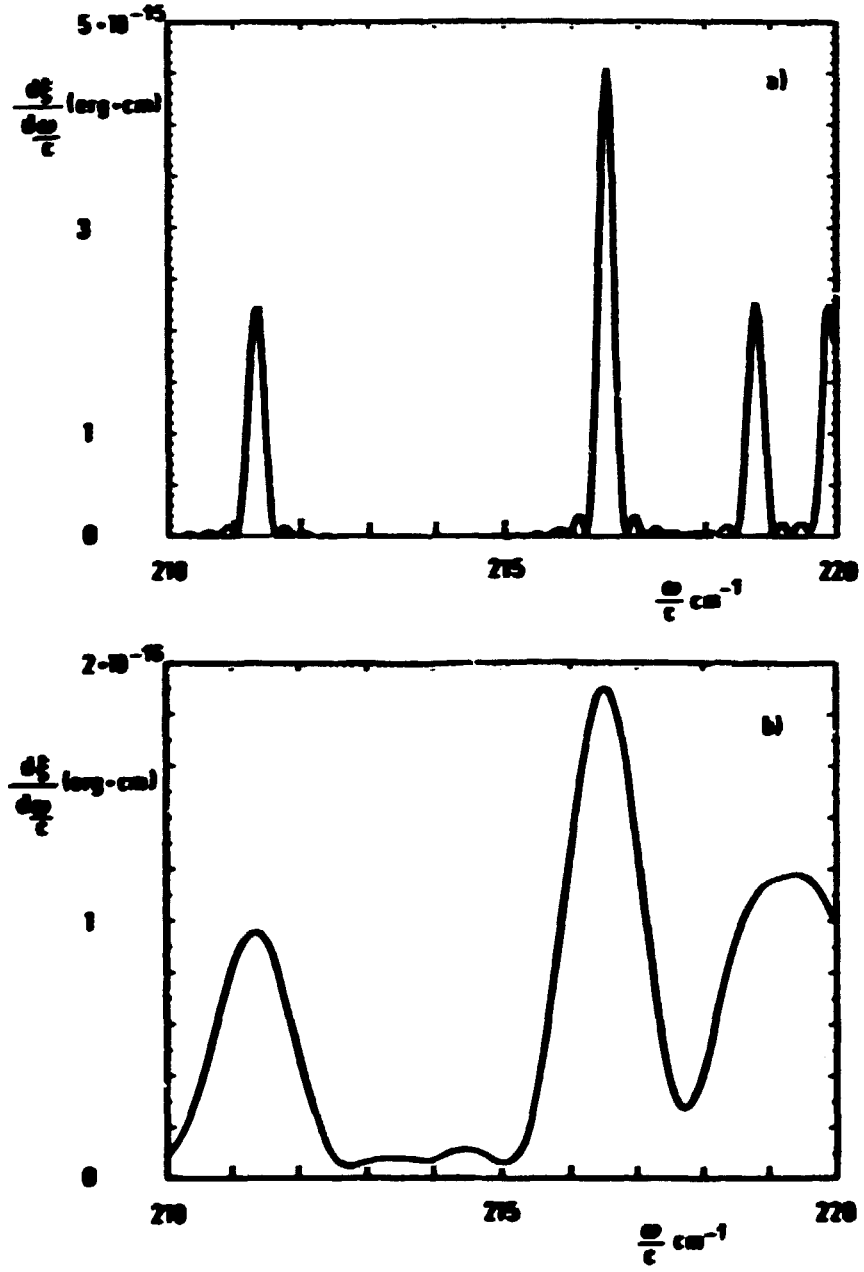

Fig. 7 On axis spectrum for a rectangular waveguide, only the odd modes are excited: (a) the excited modes are well distinguished (L=25 cm); (b) for shorter interaction length it's to be noted a remarkable interference (L=5 cm).

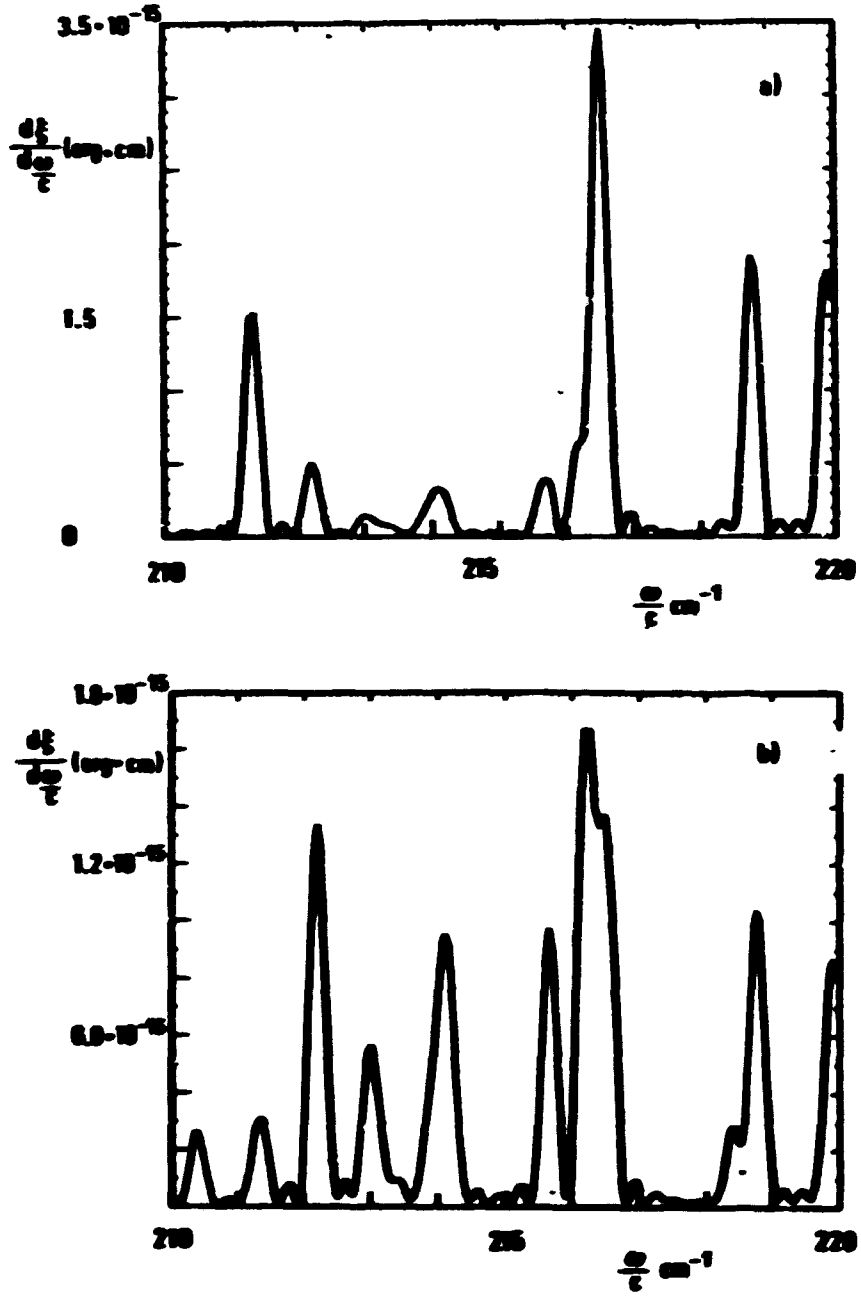

Fig. 8 Off-axis spectrum for a rectangular waveguide. Also the even modes are excited. (a) x_e=1.02 mm, y_e=1.53 mm; (b) x_e=1.04 mm, y_e=1.56 mm.

at the centre of the guide (a=2 mm, b=3 mm, β_e=0.95). The remarkable feature is the larger number of excited modes which gives, at shorter interaction length the interference pattern shown in Fig. 7b. The emission spectra for a charged particle moving parallel to the symmetry axis, but outside the centre of the guide is shown in Fig. 8. The figure exhibits an increasingly number of excited modes with an

intensity strongly dependent on the coordinates of motion of the electron.

To give an idea of the effect of the transverse e-beam distribution on the emission spectra, we have convoluted (3.10) on a transverse e-beam Gaussian distribution with r.m.s. $\sigma_{x,y}$. Many modes are excited, their spectral shape depends on the values of $\sigma_{x,y}$ and the peak intensity is decreased (Fig. 9).

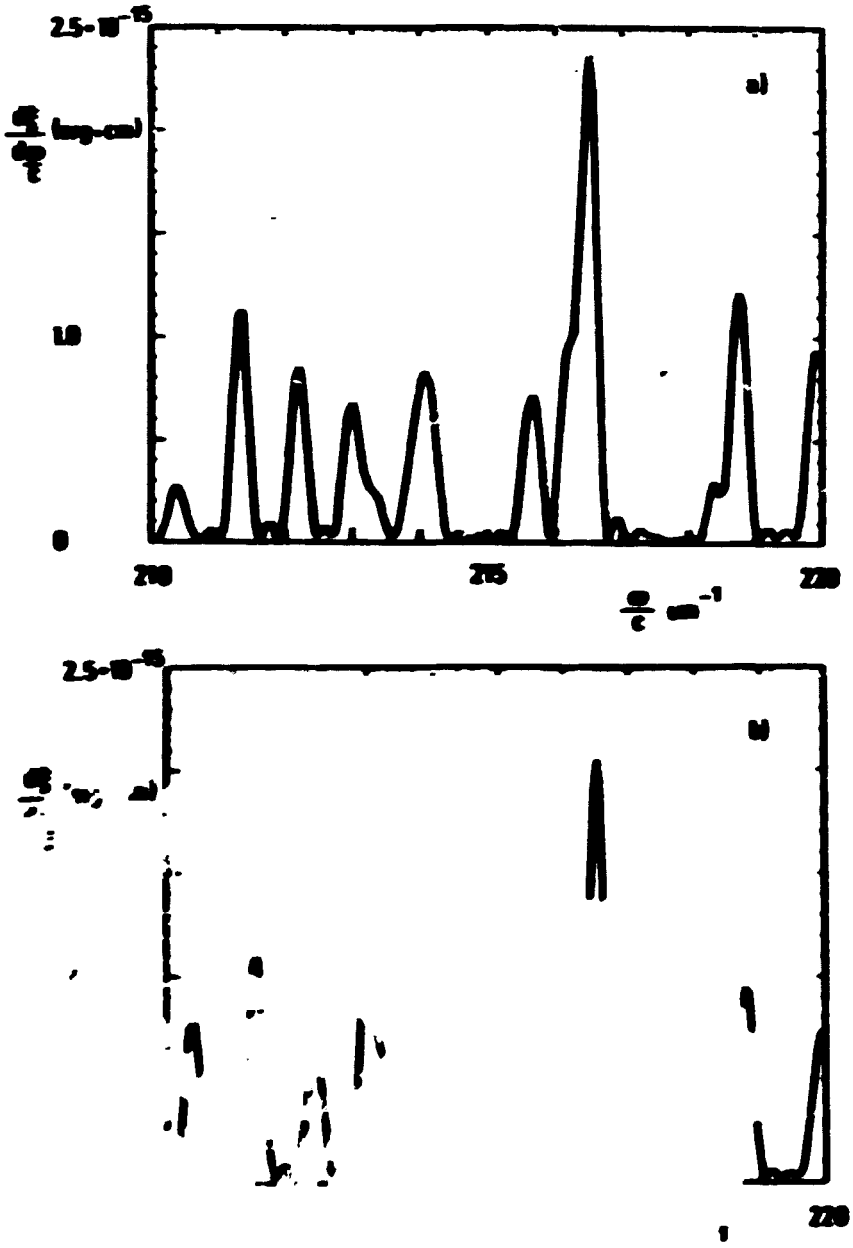

Fig. 9 [illegible] verse Gaussian distribution: a) $\sigma_{x,y}$ = 0 mm, σ_y = .075 mm; b) σ_x [illegible]

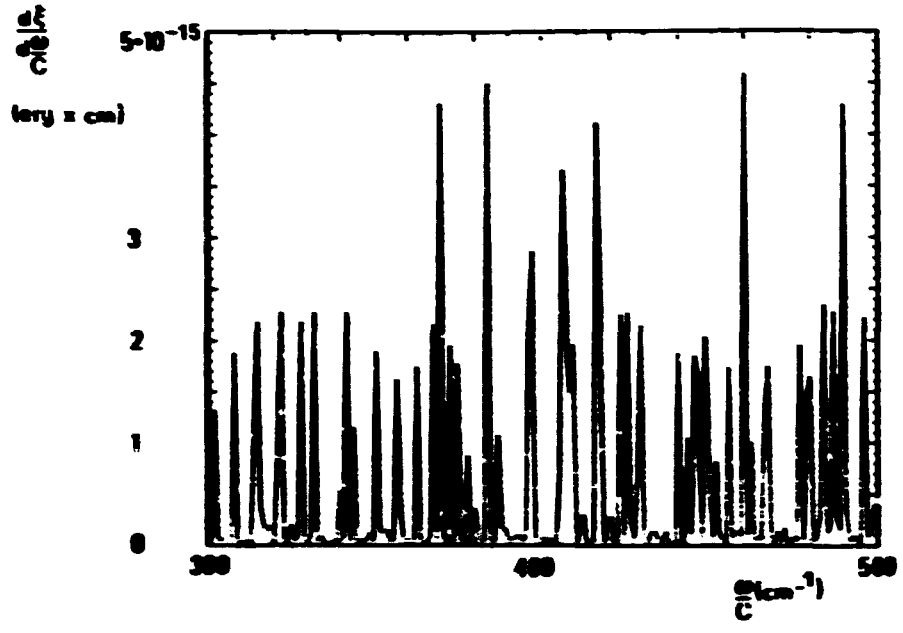

Fig. 10 A more general view of the spectrum shows the large number of excited modes.

We must finally underline that owing to the large number of excited modes a possible FEL of this type is a rather wide-band and noisy device (see also Fig. 10).

We will discuss in the next section a configuration which allows a selection of one mode and ensures, in principle, a single-mode oscillation.

IV. SLAB-CONFIGURATION

The theory so far developed has accounted for the essential features of the spectrum of the radiation emitted by a uniformly moving charge in a circular and rectangular resonator filled with a dielectric.

Two types of considerations suggest, however, the use of a different "pump-field" configuration to realise a practical C-FEL device.

The first, as already stressed, is the large number of modes simultaneously excited by the e-beam, the second, more serious, is the deterioration of the e-beam qualities as a consequence of the interaction with the dielectric, which in turn may cause a large inhomogeneous broadening and thus a significant reduction of the gain.

A possible solution is the slab configuration adopted in the

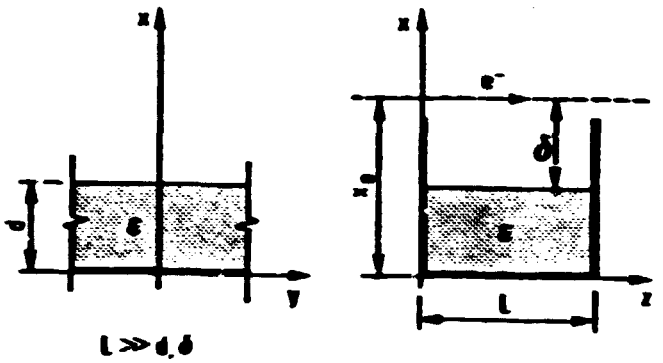

Fig. 11 Slab configuration.

"EMEA-Dartmouth" C-FEL microtron experiment (see Ref. 15), the sketch of the apparatus is shown in Fig. 11.

The amount of spontaneously radiated energy can be evaluated along the same lines developed in section 2.

The vector potential in the slab takes the form [23]

$$A_x = \phi_o \frac{ck}{\omega p} \cos(px)\sin(kz)$$
$$A_y = 0 \qquad \text{inside the dielectric} \qquad (4.1a)$$
$$A_z = \phi_o \frac{c}{i\omega} \sin(px)\sin(kz)$$

and

$$A_x = \phi'_o \frac{ck}{\omega q} e^{-qx}\sin(kz)$$
$$A_y = 0 \qquad \text{outside the dielectric} \qquad (4.1b)$$
$$A_z = \phi'_o \frac{c}{i\omega} e^{-qx}\sin(kz)$$

where

$$\phi_o^2 = \frac{16\pi c^2}{\varepsilon y_c d L(c/\omega)^2[(k/p)^2+1]} \qquad (4.2a)$$

$$\phi_o'^2 = \frac{16\pi c^2}{\varepsilon y_o L(c/\omega)^2[(k/q)^2+1]} e^{2qd} q \qquad (4.2b)$$

(y_o = maximum y transverse dimension) d is thickness of the dielectric

and p and q are related by the dispersion relations imposed by the continuity conditions and read [21]

$$qd = \frac{pd}{\varepsilon} \operatorname{tg}(pd)$$

$$(pd)^2+(qd)^2 = (\varepsilon-1)d^2(\omega/c)^2 \tag{4.3}$$

The emission wave length can be immediately obtained as the intersection of the above two curves in the (qd, pd) plane (see Fig. 12). The cut-off frequency of the TM modes is linked to the radius of the circle of Fig. 11 by the condition k = nπ. To give an example, whilst TM_0 has no cut-off frequency, when d=5 μm and ε=2 the cut-off wave-length of TM_1 is about $\lambda_c \simeq 10$ μm.

Without any change of the formalism developed in Section 2, after a somewhat tedious algebra, we can write the energy radiated per unit bandwidth in the form

$$\frac{d\mathcal{E}}{d(\omega/c)} = -\pi^2 \sum_n \frac{|\tilde{F}_n(\omega)|^2}{(k/(\omega/c)-\beta_0)} \bar{\rho}_k(\{n\},\omega) \tag{4.4}$$

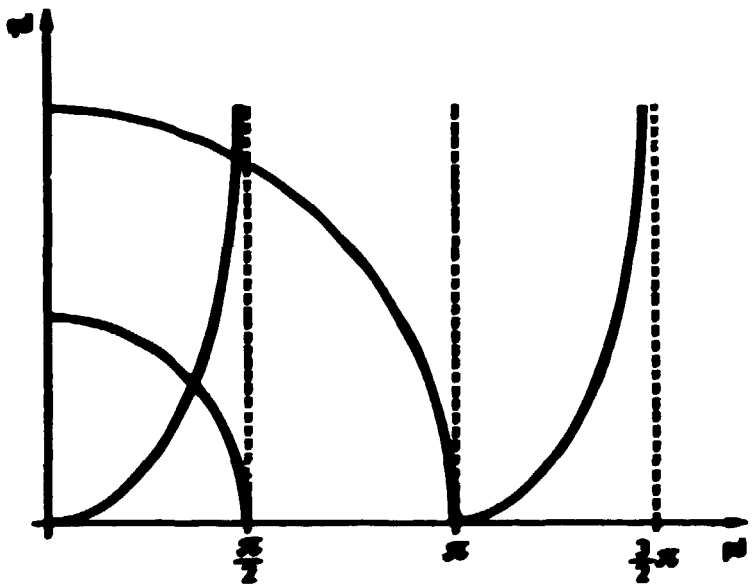

Fig. 12 The dispersion relations. The transverse wavenumbers p and q for TM_n mode are determined by the intersection between the circonference and the n-th branch of the circular tangent.

where

$$|\tilde{F}_n(\omega)|^2 = \frac{B_n^2 |C_n|^2 \, e^{-(qL\beta_\perp/\beta_o)}}{8|\phi_+||\phi_-|} \{[\frac{|\phi_+|}{|\phi_-|}(\cosh(qL\,\beta_\perp/\beta_o)-\cos 2\theta_-) +$$

$$+ \frac{|\phi_-|}{|\phi_+|}(\cosh(qL\frac{\beta_\perp}{\beta_o}) - \cos 2\theta_+)] - [e^{(qL\beta_\perp/\beta_o)}\cos\chi +$$

$$+ e^{-(qL\beta_\perp/\beta_o)}\cos(2kL+\chi) - 2\cos(\omega L/c\beta_o)\cos(kL+\chi)]\} \qquad (4.5)$$

and

$$B_n^2 = \frac{e^2C^2}{4\pi^2\omega^2}\psi_o'^2\frac{L^2}{C^2}e^{-2qx_e}\,; \qquad |C_n|^2 = 1+(\frac{\beta_\perp}{\beta_o}\frac{k}{q})^2$$

$$|\phi_-|^2 = \theta_-^2+(\frac{qL}{2}\frac{\beta_\perp}{\beta_o})^2\,; \qquad |\phi_+|^2 = \theta_+^2+(\frac{qL}{2}\frac{\beta_\perp}{\beta_o})^2$$

$$\phi_-\phi_+ = |\phi_+\phi_-|\,e^{i\chi}$$

$$|\phi_+\phi_-| = (\frac{L}{2c\beta_o})^2\sqrt{[\omega^2-(ck\beta_o)^2+(q\beta_\perp c)^2]^2+[2q\beta_\perp c^2k\beta_o]^2}$$

$$\chi = tg^{-1}\{\frac{(2q\beta_\perp c^2\,k\,\beta_o)}{[\omega^2-(ck\beta_o)^2+(q\beta_\perp c)^2]}\} \qquad (4.6)$$

θ_+ and θ_- are those defined in section 3.

The results of the numerical analysis are shown in Figs 13,14 and 15.

In Fig. 13 the energy spectrum is plotted for two different values of the electron distance from the dielectric surface (L=25 cm, β_o=0.995). At smaller electron distance the spectrum has the familiar shape, whilst for larger values a number of new peaks appear and the maximum is significantly decreased.

The central peak wavelength as a function of the dielectric thickness, the electron energy and dielectric constant ε is shown in Fig 14, and is consistent with the parametrization [23].

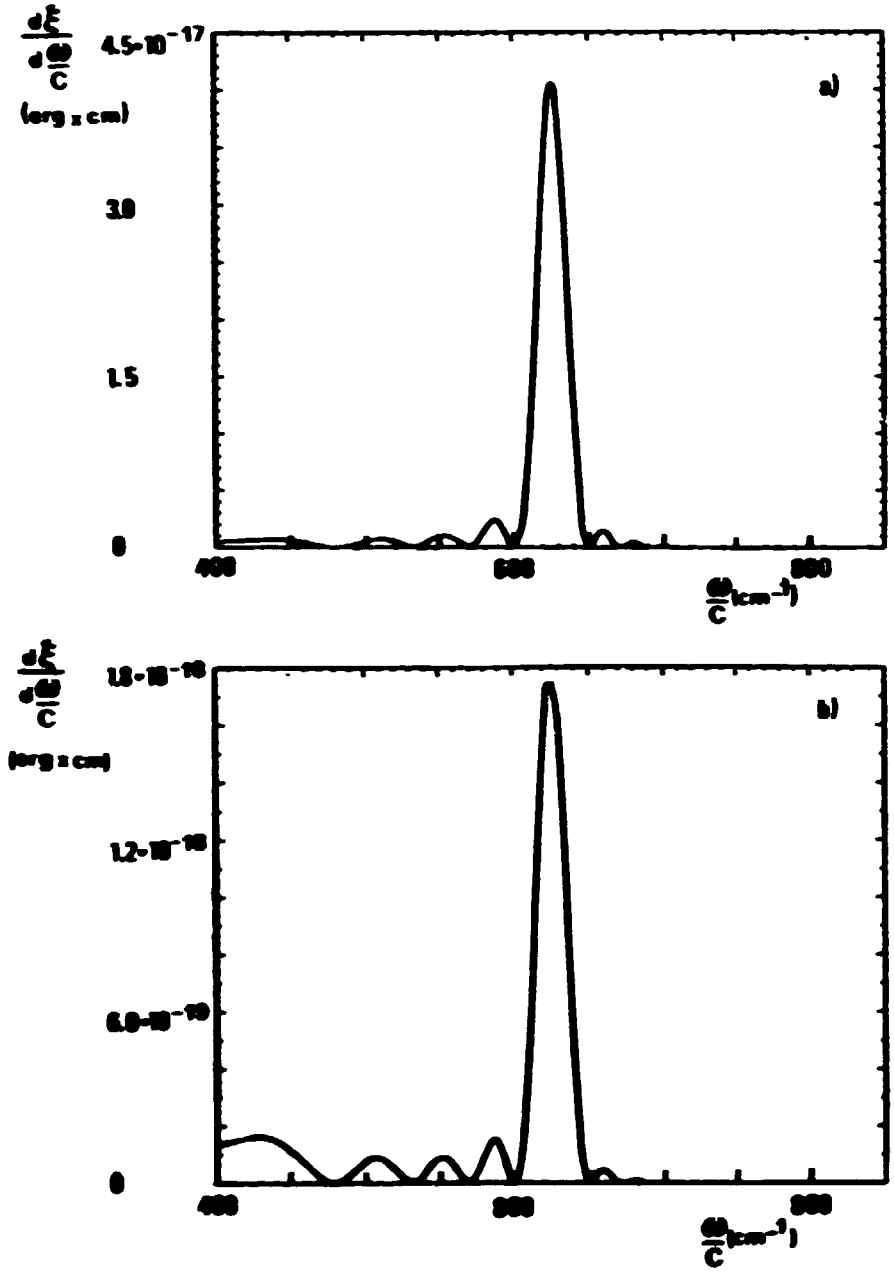

Fig. 13 Energy spectrum for the slab configuration (d=3.2 μm); (a) x_e=0.25 mm, (b) x_e=0.5 mm.

In Fig. 15 we have plotted the maximum peak intensity against the dielectric thickness, for different electron energy values. This quantity is strongly dependent on the thickness, electron energy and distance from the dielectric surface.

These preliminary results will be completed with a more careful

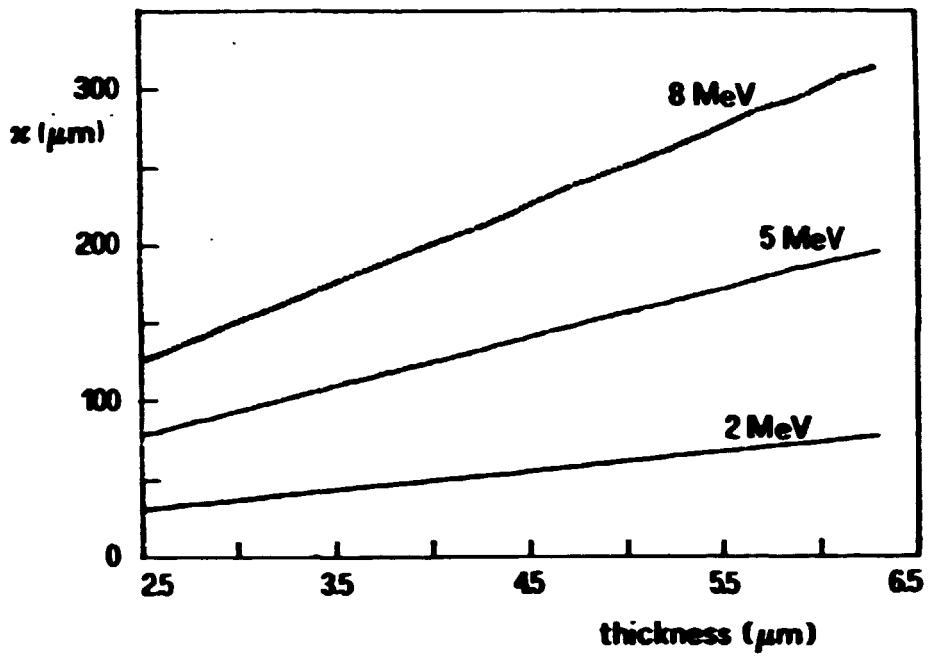

Fig. 14 Central peak wavelength as a function of dielectric thickness d, electron energy.

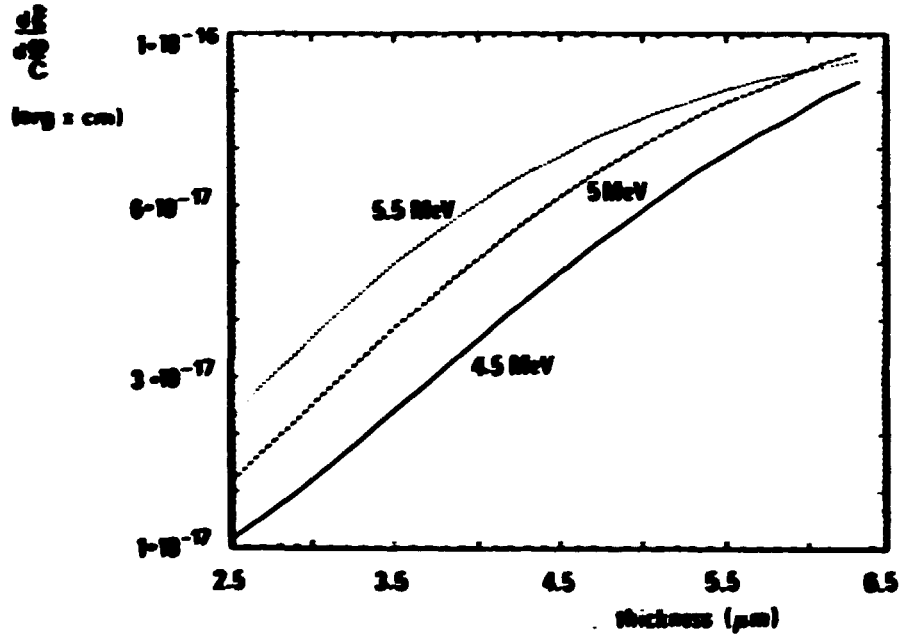

Fig. 15 Maximum peak intensity vs dielectric thickness d and electron energy.

analysis concerning the effect of the beam qualities (energy spread and emittances) in a forthcoming paper.

V. CONCLUSIONS

In this paper we have discussed an analytical method to study the spectral characteristics of the spontaneously radiated power in structures which may be, in principle, utilised for Cerenkov type FEL's.

The denomination of the so far discussed process as "spontaneous emission" may sound, strictly speaking not correct. A more appropriate denomination should be, indeed, mode excitation in bounded structures without a preexisting field. The adopted terminology, albeit not rigorous, has been chosen just to share a common language with the conventional lasers or the UFEL.

This paper has been motivated by a number of reasons, the most obvious of which was the realisation that an analysis similar to that developed for the undulators was not yet accomplished for Cerenkov type FEL's.

The study of the spontaneous emission in undulators proved a fruitful guide to get a number of indications to exploit the emission in many different ways as:

(a) The use of the higher harmonics emission (on and off axis) to get a larger laser tunability [16].

(b) The use of the undulator tapering to enhance the laser efficiency [24].

(c) The possibility of designing optical klystron (O.K.) type structures to enhance the gain [25].

(d) Useful e-beam diagnostic.

The analysis we have developed, even though preliminar, was also aimed to indicate in how many flexible ways the Cerenkov radiation may be utilised for a C-FEL device.

In a future paper we will indeed discuss the angular details of the radiation spectrum and we will also point out that, in the slab configuration, the dielectric thickness may be suitably tapered to get a large C-FEL efficiency [26].

We will also discuss the possibility of arranging two slabs to get a C-O.K. configuration and we will show that one can reproduce the same U-O.K. gain curve [27].

As to the possibility of utilising the Cerenkov emission (in the

slab configuration) as e-beam diagnostic we will show that the radiation, under appropriate conditions, can be exploited as e-beam emittance monitoring [26].

The present effort has been therefore only preliminar, we hope, however, that in the next future the spontaneous emission in C-type devices will play a role analogous to that already played in undulator magnets.

ACKNOWLEDGEMENTS

The authors owe their gratitude for stimulating discussions and enlightening comments to all the members of the "Laboratorio Laser di Potenza" of the ENEA Frascati Center.

J.E. Walsh acknowledges support of U.S. Army Research office through Grant no DAAG 29-83-k-0018.

REFERENCES

1 G. Dattoli and A. Renieri in "Laser Handbook" ed. by M.L. Stitch and M.S. Bass (North-Holland Amsterdam, 1986) 4, p. 1.

2 See the "Proceedings of the 1985 FEL Conference", Lake Tahoe, (1985) to be published.

3 Workshop "Application of FEL" ed. by A. De Angelis and D.A.G. Deacon, Nucl. Instrum. & Methods A 239,371 (1985).

4 G. Dattoli, A. Renieri and A. Torre, Proc. of the CAS School, Oxford (1985) to be published.

5 G. Dattoli, T. Letardi, J.M.J. Madey and A. Renieri, Nucl. Instrum. & Methods A 237, 326 (1985).

6 See e.g. A. Gover and P. Sprangle in "Free electron Lasers" ed. by S. Martellucci and A.N. Chester (Plenum Press 1983) p. 1.

7 A. Gover and Z. Livne, Opt. Commun. 26, 375 (1978);
J.E. Walsh, T.L. Buller, B. Johnson, G. Dattoli, F. Ciocci, IEEE J. Quantum Electron. 21, 920 (1985).

8 A. Gover and A. Yariv, Appl. Phys. 16, 121 (1978).

9 P. Coleman and C. Enderby, J. Appl. Phys. 31, 1695 (1960).

10 J.E. Walsh, T.C. Marshall and S.P. Schlesinger, Phys. Fluids 20, 709 (1977).

11 S. Von Laven, J. Branscum, J. Golub, R. Layman and J.E. Walsh, Appl. Phys. Lett. 41, 808 (1982).

12 J.A. Edighoffer, W.D. Kimura, R.H. Pantell, M.A. Piestrup, D.Y. Wang, Phys. Rev. A 23, 1848 (1981).

13 J. Murphy and J.E. Walsh, IEEE J. Quantum Electron. QE-18-8, 1259, (1982).

14 G. Dattoli, B. Johnson, A. Renieri and J.E. Walsh, Phys. Rev. Lett. 53(8), 779 (1984).

15 See J.E. Walsh in Ref. 2.

16 W.B. Colson, G. Dattoli and F. Ciocci, Phys. Rev. A 31, 828 (1985).

17 J.G. Linhart, J. Appl. Phys. 26, 527 (1955).

18 B.M. Bolotovskii, Sov. Phys. Usp. 4, 781 (1962);
A.J. Akhiezer, Doklady AN SSSR 73, 55 (1950);
A. J. Akhiezer, Lyubarskii and Fainberg, J. Tech. Phys. (USSR) 25, 2526 (1955).

19 W. Heitler "The Quantum Theory of Radiation" (Oxford University Press, 1944).

20 G. Dattoli, J.C. Gallardo and A. Torre, Phys. Rev. A 31, 3755 (1985).

21 R.E. Collin "Foundations for Microwave Engineering" (Mac Graw Hill, 1966).

22 R.H. Pantell in "Physics of Quantum Electronics" ed. by S.F Jacobs, M.S. Pilloff, M. Sargent, M.O. Scully, R. Spitzer (Addison-Wesley Publishing Company Inc. 1980) 7 p. 1.

23 B. Johnson, Ph.D Thesis-Dartmouth College, Hanover, N.H.

24 See e.g. N.M. Kroll, P.L. Morton and M.N. Rosenbluth, Phys. Q. Electronics 7, 89 (1980).

25 See e.g. P. Elleaume, J. de Physique C1, 333 (1982).

26 F. Ciocci, G. Dattoli, A. Doria, G. Schettini, A. Torre and J.E. Walsh, in preparation.

27 J.E. Walsh, G. Dattoli and F. Ciocci, in preparation.

Edito dall'ENEA, Direzione Centrale Relazioni,
Viale Regina Margherita 125, Roma.
Finito di stampare nel febbraio 1987
Fotoriproduzione e Stampa Arti Grafiche S. Marcello
V.le Regina Margherita, 176 - Roma